

GLUING DOUBLY PERIODIC SCHERK SURFACES INTO MINIMAL SURFACES

HAO CHEN AND YUNHUA WU

ABSTRACT. We construct minimal surfaces by stacking doubly periodic Scherk surfaces one above another and gluing them along their ends. It is previously known that the Karcher–Meeks–Rosenberg (KMR) doubly periodic minimal surfaces and Meeks’ family of triply periodic minimal surfaces can both be obtained by gluing two Scherk surfaces. There have been hope and failed attempts to glue more Scherk surfaces. But our analysis shows that: Except for the special case where the doubly periodic Scherk surfaces all have triangular horizontal lattice, a glue construction can only produce the trivial Scherk surface itself, the KMR examples, or Meeks’ surfaces.

1. INTRODUCTION

The goal of this paper is to glue finitely many doubly periodic Scherk surfaces into minimal surfaces.

Doubly periodic Scherk surfaces (or simply *Scherk surfaces* hereafter) form a 1-parameter family of doubly periodic minimal surfaces (DPMSSs). If we quotient out the periods, a Scherk surface \mathcal{S} is a minimal surface of genus 0 in $\mathbb{T}^2 \times \mathbb{R}$ with four vertical Scherk ends (asymptotic to vertical planes). Two of the ends extend upwards and both are parallel to $\mathbf{T}_1 = (\cos \theta_1, \sin \theta_1)$, and the other two extend downwards and both are parallel to $\mathbf{T}_2 = (\cos \theta_2, \sin \theta_2)$. Here, \mathbb{T}^2 is a flat torus whose fundamental parallelogram is a rhombus spanned by $2\pi\mathbf{T}_1$ and $2\pi\mathbf{T}_2$. \mathcal{S} is a minimal graph over the domain

$$\{a\mathbf{T}_1 + b\mathbf{T}_2 \mid (a, b) \in (0, \pi)^2 \cup (\pi, 2\pi)^2\}.$$

So it looks like a rhombic checkerboard when seen from above and \mathcal{S} is only defined over the “black” rhombi; see Figure 3. From far away, \mathcal{S} looks like vertical planes parallel to \mathbf{T}_1 suddenly transition into vertical planes parallel to \mathbf{T}_2 . The Gaussian curvature accumulates near a horizontal plane where the transition occurs.

Karcher–Meeks–Rosenberg (KMR) surfaces are DPMSSs of genus 1 with four ends that form a three-parameter family. They admit limits that look like two Scherk surfaces glued along their ends. Meeks’ family of triply periodic minimal surfaces (TPMSs) of genus 3 also admit limits that look like two Scherk surfaces glued together. For instance, Figure 1 shows Scherk limits of Schwarz’ CLP, oP, and oD families. These examples stimulate hope and (failed) attempts to glue more Scherk surfaces into minimal surfaces of higher genus.

We will show that, except for the special case of triangular horizontal lattice, one can not construct a periodic minimal surface by gluing more than two but finitely many Scherk surfaces. More precisely

Theorem 1. *Let \mathcal{M}_ε , $\varepsilon > 0$, be a one-parameter family of minimal surfaces in $\mathbb{T}_\varepsilon^2 \times \mathbb{R}$ such that, as $\varepsilon \rightarrow 0$ and for any $H \in \mathbb{R}$, $\mathcal{M}_\varepsilon - (0, 0, H/\varepsilon^2)$ converges either to a doubly periodic Scherk surface, or to a pair of vertical planes. Then*

Date: September 2, 2025.

2010 Mathematics Subject Classification. Primary 53A10.

Key words and phrases. minimal surfaces.

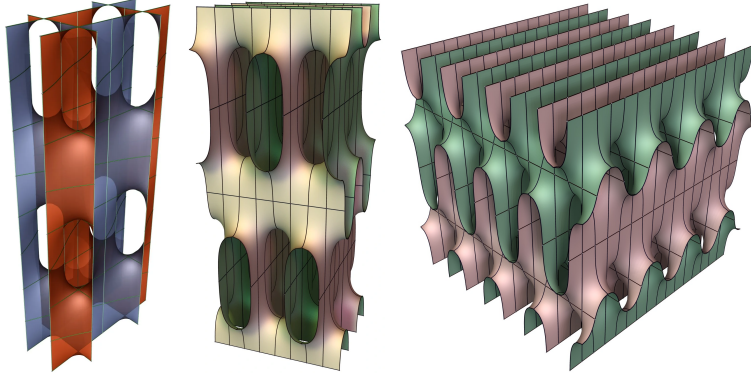


FIGURE 1. Triply periodic CLP (left), oP (middle), and oD (right) surfaces near the doubly periodic Scherk limit.

- either the horizontal flat torus \mathbb{T}_ε^2 converges to a triangular lattice as $\varepsilon \rightarrow 0$,
- or otherwise, for ε sufficiently small, \mathcal{M}_ε is either a doubly periodic Scherk surface, a KMR example, or a member of the Meeks family.

We must stress that, by a “doubly periodic Scherk surface in $\mathbb{T}^2 \times \mathbb{R}$ ”, we only mean the DPMS of genus 0 with four Scherk ends. Otherwise, one could always choose a larger horizontal flat torus to achieve a higher genus. This will bring more flexibility to the gluing construction. This is however not considered in the current paper.

Then the triangular lattice turns out to be the only horizontal lattice that could produce higher-genus examples. In fact, a recent numeric study has constructed a TPMS of genus 4 with a limit that looks like three Scherk surfaces glued together, and the horizontal lattice is indeed triangular [5]. A rigorous proof for this example is under preparation. Even more complicated examples is possible with the triangular horizontal lattice; see Remark 3. However, this special case is not the focus of the current paper. We will mainly talk about the “otherwise” part of Main Theorem 1.

This paper is one in a series that aims to completely describe the ideal boundary of the moduli space of the TPMSs of genus 3. Previously, TPMSs of genus 3 have been constructed by gluing catenoids, helicoids, and simply periodic Scherk surfaces [9, 1, 2].

1.1. Glue Scherk surfaces into TPMSs. We first try to construct TPMSs that look like n Scherk surfaces, say $\mathcal{S}_1, \mathcal{S}_2, \dots, \mathcal{S}_n$, stacked one above another and *periodically* glued along their ends. More precisely, for $1 \leq k \leq n$, the upward ends of \mathcal{S}_k are glued with the downward ends of \mathcal{S}_{k+1} , where the subscript is taken modulo n (same afterwards). It is then necessary that $n = 2m$ is even and (the asymptotic planes of) the upward ends of \mathcal{S}_k and the downward ends of \mathcal{S}_{k+1} are parallel.

In the current paper, we only consider the simple case where the ends take only two directions, depending on the parity of k . For this purpose, we define the parity function

$$\varsigma(k) = \begin{cases} 1, & k \text{ odd}, \\ 2, & k \text{ even}, \end{cases}$$

and we assume that the upward (resp. downward) ends of \mathcal{S}_k are parallel to $\mathbf{T}_{\varsigma(k)}$ (resp. $\mathbf{T}_{\varsigma(k-1)}$). This assumption seems to be an oversimplification, but is actually generally true. We will prove that

Lemma 2. *Under the assumptions of Theorem 1,*

- either the horizontal flat torus \mathbb{T}_ε^2 converges to a triangular lattice as $\varepsilon \rightarrow 0$, and the limit vertical planes have three possible directions,
- or otherwise, the vertical planes alternate between two possible directions.

The surfaces we plan to construct form families \mathcal{M}_ε parameterized by a real parameter ε . At the beginning, $\varepsilon = 0$ and the \mathcal{S}_k 's are infinite distance apart. Between \mathcal{S}_k and \mathcal{S}_{k+1} , the surface \mathcal{M}_0 appears as vertical planes parallel to $\mathbf{T}_{\varsigma(k)}$. After a scaling by ε^2 , the distances between the \mathcal{S}_k 's become finite, but the vertical planes become infinitesimally close. The Gaussian curvature explodes at horizontal planes where the directions of the vertical planes suddenly change. Let h_k denote the heights of these horizontal planes, which can be seen as the height of \mathcal{S}_k . Then $\varepsilon^2 \mathcal{M}_\varepsilon$ looks like foliations of $\mathbb{T}^2 \times (h_k, h_{k+1})$ by vertical planes. We define $\ell_k = h_{k+1} - h_k$, $1 \leq k \leq n$, as the scaled distance between the \mathcal{S}_k and \mathcal{S}_{k+1} , and write $\ell = (\ell_k)_{1 \leq k \leq n}$ as a finite sequence of length n . Up to a reparameterization and a rescaling, we may assume that $\sum_k \ell_k = 1$.

Moreover, it is possible that \mathcal{S}_{k+1} “slides” with respect to \mathcal{S}_k along the glued end. The amount of the sliding, termed “phase difference” and denoted ψ_k , is defined as follows: When the domain of \mathcal{S}_{k+1} as a minimal graph coincides with the domain of \mathcal{S}_k , the phase difference of \mathcal{S}_{k+1} with respect to \mathcal{S}_k is $\psi_k = 0$, and we say \mathcal{S}_{k+1} is *in phase* with \mathcal{S}_k ; see Figure 2 (left). In general, \mathcal{S}_{k+1} is translated from the in-phase position by a vector $\psi_k \mathbf{T}_{\varsigma(k)}$, where $\psi_k \in \mathbb{R}/2\pi\mathbb{Z}$ is the phase difference. Note that, when $\psi_k = \pi$, the closures of the domains of \mathcal{S}_k and \mathcal{S}_{k+1} cover the plane; in this case, we say that \mathcal{S}_{k+1} is *in opposite phase* with \mathcal{S}_k ; see Figure 2 (right). The sequence $\psi = (\psi_k)_{1 \leq k \leq n}$ is again a finite sequence of length n .

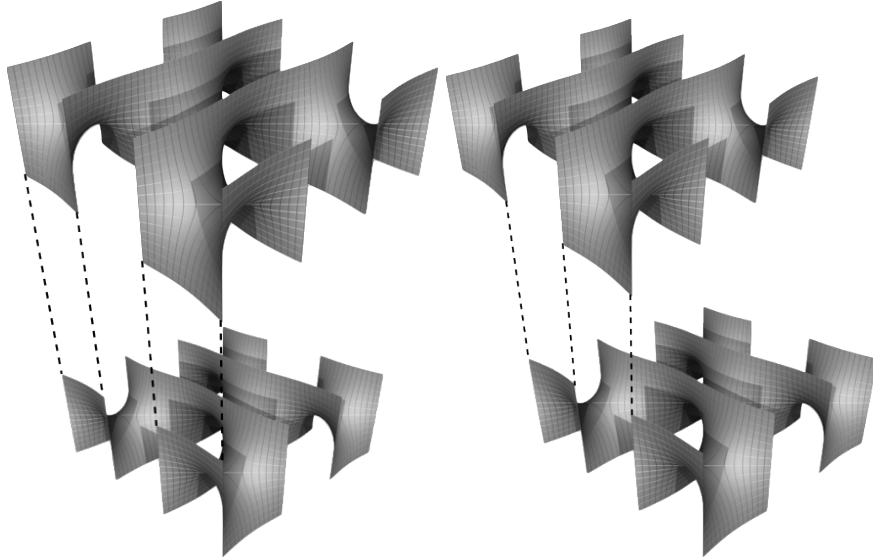


FIGURE 2. Two doubly periodic Scherk surfaces glued at phase 0 (left) and phase π (right).

The pair (ℓ, ψ) is termed a *configuration*. They give a complete description of the gluing pattern.

As ε increases, the idea of the gluing is to desingularize the initial surface. There are two ways to look at the desingularization. Either the \mathcal{S}_k 's are pulled a little bit

closer towards each other, hence the distances between them are reduced. Alternatively, after a scaling by ε^2 , the vertical planes are pushed a little bit away from each other, hence the horizontal periods increase.

Our construction allows the horizontal flat torus to differ from rhombic after desingularization. Hence the horizontal periods, initially $2\pi\mathbf{T}_1$ and $2\pi\mathbf{T}_2$ for $\varepsilon = 0$, may not be unit vectors for $\varepsilon > 0$. Define

$$\ell_{\max} = \max_k \ell_k, \quad \tau_{\max} = \exp(-\ell_{\max}/\varepsilon^2).$$

We assume that the horizontal periods are of the form

$$(1) \quad 2\pi\mathbf{T}_1(1 + \Lambda_1\tau_{\max}), \quad 2\pi\mathbf{T}_2(1 + \Lambda_2\tau_{\max}),$$

where Λ_1 and Λ_2 are real numbers. See the proof of Proposition 7 for the motivation of this assumption. Note that, as $\tau \rightarrow 0$, the aspect ratio is

$$\frac{1 + \Lambda_1\tau_{\max}}{1 + \Lambda_2\tau_{\max}} = 1 + (\Lambda_1 - \Lambda_2)\tau_{\max} + o(\tau_{\max}).$$

So the aspect ratio is determined to the first order by $\Lambda_1 - \Lambda_2$. Adding the same constant to both Λ corresponds to a scaling of the horizontal lattice to the first order.

Define

$$\Psi_1 = \sum_{j=1}^{n/2} \psi_{2j-1}, \quad \Psi_2 = \sum_{j=1}^{n/2} \psi_{2j}, \quad \mathbf{T}_3 = \Psi_1\mathbf{T}_1 + \Psi_2\mathbf{T}_2,$$

Then $\mathbf{T}_3 + (\Psi_1\Lambda_1\mathbf{T}_1 + \Psi_2\Lambda_2\mathbf{T}_2)\tau_{\max}$ is the horizontal component of the "vertical" period, while $1/\varepsilon^2$ is the horizontal component.

To summarise: Given a periodic configuration (ℓ, ψ) of length $n = 2m$. We expect, for sufficiently small $\varepsilon > 0$, a family \mathcal{M}_ε of minimal surfaces of genus $n+1$, in the flat torus

$$(2) \quad \mathbb{T}_\varepsilon^3 = \mathbb{R}^3 / 2\pi \langle (\mathbf{T}_1(1 + \Lambda_1\tau_{\max}), 0), (\mathbf{T}_2(1 + \Lambda_2\tau_{\max}), 0), \\ (\mathbf{T}_3 + (\Psi_1\Lambda_1\mathbf{T}_1 + \Psi_2\Lambda_2\mathbf{T}_2)\tau_{\max}, 1/\varepsilon^2) \rangle.$$

They lift to TPMSSs $\tilde{\mathcal{M}}_\varepsilon$ in \mathbb{R}^3 such that

- For each $1 \leq k \leq n$, there exists functions $H_k(\varepsilon)$ that diverges to infinity while $\mathcal{M}_\varepsilon - (0, 0, H_k(\varepsilon))$ converges to a doubly periodic Scherk surface \mathcal{S}_k as $\varepsilon \rightarrow 0$. Moreover, $\varepsilon^{-2}(H_{k+1} - H_k) \rightarrow \ell_k$ as $\varepsilon \rightarrow 0$.
- As $\varepsilon \rightarrow 0$, $\tilde{\mathcal{M}}_\varepsilon$ converges, after a scaling by ε^2 , to foliations by vertical planes of the direct product of \mathbb{R}^2 with segments of length ℓ_k .
- As $\varepsilon \rightarrow 0$, the phase difference between \mathcal{S}_{k+1} and \mathcal{S}_k converges to ψ_k .

In general, for such a gluing construction to succeed, a balance condition is necessary, and a non-degenerate condition is needed for the use of the Implicit Function Theorem. In the current construction, the balance condition requires that ℓ_k and ψ_k only depend on the parity of k . That is,

$$(\ell_k, \psi_k) = (\ell_{\varsigma(k)}, \psi_{\varsigma(k)}).$$

We will also require that

$$K_k = \begin{cases} 4\cos(\psi_k) + \Lambda_{\varsigma(k)} \exp(\zeta_k), & \ell_k = \ell_{\max}, \\ 4\cos(\psi_k), & \ell_k < \ell_{\max}, \end{cases}$$

is nonzero for all $1 \leq k \leq n$, where $\zeta_k = \partial\ell_k/\partial(\varepsilon^2)$. This condition is not here to allow the use of the Implicit Function Theorem, but it does allow us to proceed with the construction.

Our main result about TPMSSs is the following

Theorem 3. *For the family \mathcal{M}_ε of triply periodic minimal surfaces described above to exist, it is necessary that*

$$(\ell_k, \psi_k) = (\ell_{\varsigma(k)}, \psi_{\varsigma(k)}).$$

If this is indeed the case and $K_k \neq 0$ for all $1 \leq k \leq n$, then ℓ is necessarily constant, and \mathcal{M}_ε does exist for sufficiently small ε and coincides with the Meeks' family of triply periodic minimal surfaces of genus 3.

The Meeks' family form a 5-dimensional real manifold, which is compatible to the 5-dimensional deformation space of the lattice. However, near the Scherk limit, the manifold is not parameterized by the shapes of the lattice. We will see in Remark 2 that $\zeta_{1,2}$ replace $\Lambda_{1,2}$ as parameters of the Meeks' manifold.

1.2. Glue Scherk surfaces into DPMSSs. Now we try to stack only a finite sequence of Scherk surfaces and construct DPMSSs, leaving four free Scherk ends that are not glued, two upwards and two downwards. More precisely: Given a configuration (ℓ, ψ) consisting of two finite sequences of the same length. We expect, for sufficiently small $\varepsilon > 0$, a family \mathcal{M}_ε of minimal surfaces of genus $n-1$ in $\mathbb{T}_\varepsilon^2 \times \mathbb{R}$ with four Scherk ends, where the flat 2-torus

$$\mathbb{T}_\varepsilon^2 = \mathbb{R}^2 / 2\pi \langle \mathbf{T}_1(1 + \Lambda_1 \tau_{\max}), \mathbf{T}_2(1 + \Lambda_2 \tau_{\max}) \rangle.$$

They lift to DPMSSs $\tilde{\mathcal{M}}_\varepsilon$ in \mathbb{R}^3 such that

- For each $1 \leq k < n$, there exists $H_k(\varepsilon)$ that diverges to infinity while $\mathcal{M}_\varepsilon - (0, 0, H_k(\varepsilon))$ converges to a doubly periodic Scherk surface \mathcal{S}_k as $\varepsilon \rightarrow 0$. Moreover, $\varepsilon^{-2}(H_{k+1} - H_k) \rightarrow \ell_k$ as $\varepsilon \rightarrow 0$.
- As $\varepsilon \rightarrow 0$, $\tilde{\mathcal{M}}_\varepsilon$ converges, after a scaling by ε^2 , to foliations by vertical planes of the direct product of \mathbb{R}^2 with segments of length ℓ_k , $1 \leq k < n$.
- As $\varepsilon \rightarrow 0$, the phase difference between \mathcal{S}_{k+1} and \mathcal{S}_k converges to ψ_k .

The technique for constructing TPMSSs applies with little change. But the balance condition is even more strict: ℓ and ψ can only be sequences of length ≤ 2 .

Theorem 4. *The family \mathcal{M}_ε of doubly periodic minimal surfaces described above exists if and only if ℓ and ψ are sequences of length 1 or 2. If they are of length 1, then \mathcal{M}_ε is the doubly periodic Scherk surface. If they are of length 2, then \mathcal{M}_ε is the Karcher–Meeks–Rosenberg examples obtained by gluing two doubly periodic Scherk surfaces.*

The paper is organized as follows: We will first review the construction and geometry of the doubly periodic Scherk surfaces in Section 2. Section 3 is the major part of this paper, where we will glue Scherk surfaces into TPMSSs. Many steps in the construction are similar to [2] hence will not be detailed. Proposition 7 and Section 3.3.3 are however key and new ingredients of the construction and will be treated very carefully. Finally, we prove Lemma 2 and Theorems 3 and 4, in this order, in Section 4. This then concludes the proof of the Main Theorem 1. The construction for DPMSSs is very similar to that of TPMSSs, hence will only be mentioned in Section 4.

Acknowledgement. The authors thank Matthias Weber, Martin Traizet, and Peter Connor for helpful discussions. The first author thanks Gerd Schroeder-Turk for hosting him at Murdoch University and for working together on the TPMSS of genus 4 with doubly Scherk limit. Some figures in this paper are from Weber's website <https://minimalsurfaces.blog/>.

2. DOUBLY PERIODIC SCHERK SURFACES

A doubly periodic Scherk surface \mathcal{S} can be constructed as follows: Let P be a rhombus spanned by two vectors of length π , say,

$$\pi\mathbf{T}_1 = \pi(\cos\theta_1, \sin\theta_1) \quad \text{and} \quad \pi\mathbf{T}_2 = \pi(\cos\theta_2, \sin\theta_2).$$

Up to a horizontal rotation, we may assume that $0 < \theta = \theta_1 = \pi - \theta_2 < \pi/2$. The Jenkins–Serrin Theorem [3] guarantees a minimal graph over P , unique up to vertical translations, that takes the value $-\infty$ along the edges of P parallel to \mathbf{T}_1 , and $+\infty$ along the edges parallel to \mathbf{T}_2 . This minimal graph is bounded by the four vertical lines over the vertices of P . Order-2 rotations around these vertical lines extend the graph into a DPMS, which is a *doubly periodic Scherk surface* \mathcal{S} with periods $2\pi\mathbf{T}_1$ and $2\pi\mathbf{T}_2$. See Figure 3.

The Weierstrass parameterization of \mathcal{S} is given by

$$z \mapsto \int_0^z (\Phi_1, \Phi_2, \Phi_3),$$

with the Weierstrass data

$$\Phi_1 = \sum_{j=1}^4 \frac{-i \cos \theta_j}{z - p_j}, \quad \Phi_2 = \sum_{j=1}^4 \frac{-i \sin \theta_j}{z - p_j}, \quad \Phi_3 = \sum_{j=1}^4 \frac{\sigma_j}{z - p_j} dz$$

defined on the Riemann sphere $\hat{\mathbb{C}}$ punctured at p_j , $1 \leq j \leq 4$, where $\sigma_j = -(-1)^j$, and θ_j are horizontal directions of the ends with

$$\theta_1 = \theta, \quad \theta_2 = \pi - \theta, \quad \theta_3 = -\pi + \theta, \quad \theta_4 = -\theta, \quad 0 < \theta < \pi/2.$$

So the ends corresponding to p_1 and p_3 extend upwards and are parallel to \mathbf{T}_1 , while the ends corresponding to p_2 and p_4 extend downwards and are parallel to \mathbf{T}_2 . See Figure 5.

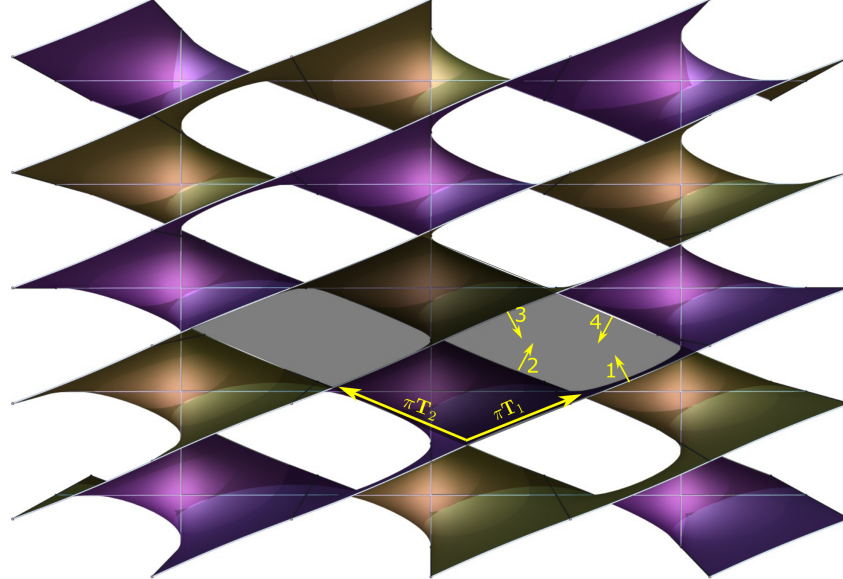


FIGURE 3. Top view of a doubly periodic Scherk surface. The grey rhombus covers a fundamental domain of the translational symmetries, spanned by $2\pi\mathbf{T}_1$ and $2\pi\mathbf{T}_2$. The four ends and their normal vectors are marked with numbers, corresponding to the subscript j in the text.

The order-2 rotations around vertical lines correspond to an anti-holomorphic involution ρ that preserves all the punctures. For convenience, we assume that the punctures all lie on the unit circle, then $\rho(z) = 1/\bar{z}$. \mathcal{S} also contains two horizontal straight lines orthogonal to each other, order-2 rotations around which interchange the upward and downward ends. They can be assumed to correspond to reflections in the real and imaginary axes. So the punctures must be symmetrically placed on the unit circle. See Figure 4 We may choose

$$-1/p_1 = p_2 = 1/p_3 = -p_4 = \exp(i\vartheta).$$

with $0 < \vartheta < \pi/2$. Then the real line of $\hat{\mathbb{C}}$ is mapped to the y -axis, and the imaginary line to the x -axis. The conformality condition $\Phi_1^2 + \Phi_2^2 + \Phi_3^2 = 0$ gives $\vartheta = \pi/2 - \theta$. Then our choice leads to a very convenient (stereographically projected) Gauss map

$$G = -\frac{\Phi_1 + i\Phi_2}{\Phi_3} = z,$$

which extends holomorphically to the punctures. So the normal vectors at the ends are

$$N(p_j) = \sigma_j(-\sin \theta_j, \cos \theta_j, 0).$$

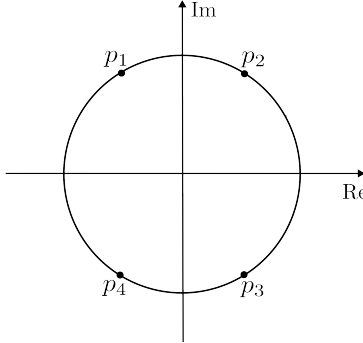


FIGURE 4. A doubly periodic Scherk surface is parameterized on a Riemann sphere with four punctures on the unit circle.

Let $w_j = i(z - p_j)/(z + p_j)$ be a local coordinate around p_j . Note that w_j is real positive on the circular segment between p_j and p_{j+1} (subscript modulo 4) and

$$w_j \circ \rho(z) = i \frac{1/\bar{z} - p_j}{1/\bar{z} + p_j} = i \frac{\bar{p}_j - \bar{z}}{\bar{p}_j + \bar{z}} = \overline{w_j(z)}$$

and, under this local coordinate, we have for $i = 1$ and 2 ,

$$\rho^* \left(\frac{\Phi_i}{w_j} \right) = -\frac{\bar{\Phi}_i}{\bar{w}_j},$$

so $\text{Res}(\Phi_i/w_j, p_j) \in i\mathbb{R}$ is pure imaginary.

The four arcs between the punctures are mapped to the four vertical lines; see Figure 5. Let

$$(\text{Re } \mu_j, \text{Im } \mu_j) := \lim_{z \rightarrow p_j} \left(-\cos(\theta_j) \arg(w_j) + \text{Re} \int_0^z \Phi_1, -\sin(\theta_j) \arg(w_j) + \text{Re} \int_0^z \Phi_2 \right)$$

be the horizontal coordinates of the image of the arc between p_j and p_{j+1} (subscript modulo 4). Then

$$\mu_1 = \pi \cos \theta, \quad \mu_2 = \pi i \sin \theta, \quad \mu_3 = -\pi \cos \theta, \quad \mu_4 = -\pi i \sin \theta,$$

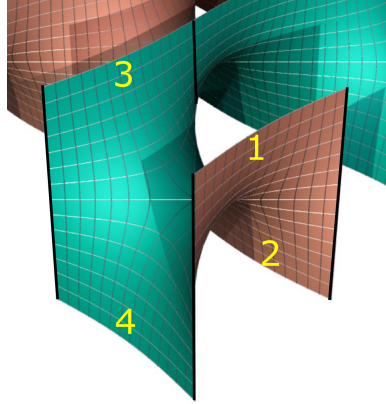


FIGURE 5. Part of a doubly periodic Scherk surface where the ends are marked and the vertical lines are highlighted.

are at the vertices of a rhombus.

Expansion of the Weierstrass parameterization around p_j in terms of w_j gives

$$\begin{aligned} \operatorname{Re} \int_0^z \Phi_1 &= \underbrace{\operatorname{Re} \mu_j + \cos \theta_j \arg(w_j(z))}_{\text{planar terms}} + \underbrace{\operatorname{Re} \left(w_j(z) \operatorname{Res} \left(\frac{\Phi_1}{w_j}, p_j \right) \right)}_{\text{undulation terms}} + O(|w_j(z)|^2), \\ \operatorname{Re} \int_0^z \Phi_2 &= \operatorname{Im} \mu_j + \sin \theta_j \arg(w_j(z)) + \operatorname{Re} \left(w_j(z) \operatorname{Res} \left(\frac{\Phi_2}{w_j}, p_j \right) \right) + O(|w_j(z)|^2), \\ \operatorname{Re} \int_0^z \Phi_3 &= \nu_j + \sigma_j \log |w_j(z)| + O(|w_j(z)|), \end{aligned}$$

where

$$\nu_j = \lim_{z \rightarrow p_j} \left(-\sigma_j \log |w_j(z)| + \operatorname{Re} \int_0^z \Phi_3 \right) = -\sigma_j \log(\sin(\theta) \cos(\theta)).$$

This shows that the ends are asymptotic to vertical planes, but also undulate with an amplitude that decays exponentially as the height tends to $\pm\infty$. See Figure 5. We then compute the “initial” amplitude in the normal directions

$$\begin{aligned} \Upsilon_j &= \sigma_j \left\langle N(p_j), \operatorname{Res} \left(\frac{\Phi}{w_j}, p_j \right) \right\rangle_H \\ &= i \sin \theta_j \operatorname{Res} \left(\frac{\Phi_1}{w_j}, p_j \right) - i \cos \theta_j \operatorname{Res} \left(\frac{\Phi_2}{w_j}, p_j \right) = 2. \end{aligned}$$

This could be more easily done using $G = z$ and noticing that

$$\Upsilon_j = \frac{i}{G} \frac{dG}{dw_j}(p_j).$$

When we glue a sequence of Scherk surfaces, the \mathcal{S} constructed above will be used to model odd-labeled Scherk surfaces \mathcal{S}_{2k-1} . As for the even-labeled Scherk surfaces \mathcal{S}_{2k} , we want that the ends corresponding to p_1 and p_3 are still upwards but parallel to \mathbf{T}_2 , the ends corresponding to p_2 and p_4 are still downwards but parallel to \mathbf{T}_1 , and that the Gauss map coincides with \mathcal{S} at the punctures but has a pole at 0. They will be modeled by a Scherk surface $\tilde{\mathcal{S}}$ with the Weierstrass data

$$\tilde{\Phi}_1 = \sum_{j=1}^4 \frac{-i \cos \tilde{\theta}_j}{z - \tilde{p}_j}, \quad \tilde{\Phi}_2 = \sum_{j=1}^4 \frac{-i \sin \tilde{\theta}_j}{z - \tilde{p}_j}, \quad \tilde{\Phi}_3 = \sum_{j=1}^4 \frac{\tilde{\sigma}_j}{z - \tilde{p}_j} dz,$$

where $\tilde{\theta}_j = \pi - \theta_j$, $\tilde{\sigma}_j = \sigma_j$, and $\tilde{p}_j = p_j$. Then the Gauss map $\tilde{G} = 1/G = 1/z$, and $G(p_j) = \tilde{G}(\tilde{p}_{5-j})$ as we expect. Hence the end of \mathcal{S} corresponding to p_j will be glued to the end of $\tilde{\mathcal{S}}$ corresponding to \tilde{p}_{5-j} . Moreover, we will use the local coordinates $\tilde{w}_j = -i(z - \tilde{p}_j)/(z + \tilde{p}_j)$. This choice is consistent with the definition of phase. Then we have

$$\tilde{\Upsilon}_j = \Upsilon_j = 2, \quad \tilde{\mu}_j = \mu_{5-j}, \quad \tilde{\nu}_j = \nu_j.$$

Note that here, $\tilde{\mu}_j$ gives the horizontal position of the arc between \tilde{p}_j and \tilde{p}_{j-1} .

3. CONSTRUCTION OF TRIPLY PERIODIC MINIMAL SURFACES

In the following, all parameters vary around a central value. The central value of a parameter x is denoted by an x° . In particular, we fix a configuration (ℓ°, ψ°) and three horizontal vectors

$$\mathbf{T}_1 = \exp(i\theta_1), \quad \mathbf{T}_2 = \exp(i\theta_2) \quad \text{and} \quad \mathbf{T}_3 = \Psi_1 \mathbf{T}_1 + \Psi_2 \mathbf{T}_2,$$

with $\theta_1 = \pi - \theta_2 = \theta$. Moreover, we define $\vartheta = \pi/2 - \theta$.

3.1. Opening nodes. Each Scherk surface \mathcal{S}_k is parameterized on a Riemann sphere $\hat{\mathbb{C}}_k$, $1 \leq k \leq n = 2m$, with four punctures on the unit circle corresponding to the ends. Unlike in the previous section, we use $p_{s,k}$ (resp. $q_{s,k}$), $s \in \{+, -\}$, to denote the punctures corresponding to the upward (resp. downward) ends, and write $p = (p_{s,k})_{s=\pm, 1 \leq k \leq n}$ and $q = (q_{s,k})_{s=\pm, 1 \leq k \leq n}$.

Our initial surface at $\varepsilon = 0$ is a noded Riemann surface Σ_0 obtained by identifying punctures $p_{s,k}$ with $q_{s,k+1}$ for $1 \leq k \leq n$, $s = \pm$. Here and afterwards, the subscripts are taken modulo n . The central values for the punctures are defined by

$$-1/p_{+,k}^\circ = q_{-,k}^\circ = 1/p_{-,k}^\circ = -q_{+,k}^\circ = \exp(i\vartheta).$$

As ε increases, we open the nodes as follows: Depending on the parity of k , consider local coordinates

$$u_{s,k} = (-1)^k i \frac{z - p_{s,k}}{z + p_{s,k}}, \quad v_{s,k} = (-1)^k i \frac{z - q_{s,k}}{z + q_{s,k}},$$

in a neighborhood of the punctures. We fix a small number $\delta > 0$ independent of k and s such that, when the punctures are at their central values, the disks $|u_{s,k}^\circ| < 2\delta$ and $|v_{s,k}^\circ| < 2\delta$ are disjoint in each Riemann sphere $\hat{\mathbb{C}}_k$. Then for punctures sufficiently close to their central values, the disks $|u_{s,k}| < \delta$ and $|v_{s,k}| < \delta$ are disjoint in each $\hat{\mathbb{C}}_k$.

Consider complex parameters $t_{s,k}$, where $1 \leq k \leq n$ and $s = \pm$. For $t = (t_{s,k})$ in the neighborhood of $t^\circ = 0$ with $0 < |t_{s,k}| < \delta^2$. We remove the disks

$$|u_{s,k}| < |t_{s,k}|/\delta, \quad |v_{s,k+1}| < |t_{s,k}|/\delta$$

and identify the annuli

$$|t_{s,k}|/\delta \leq |u_{s,k}| \leq \delta \quad \text{and} \quad |t_{s,k}|/\delta \leq |v_{s,k+1}| \leq \delta$$

by

$$u_{s,k} v_{s,k+1} = t_{s,k},$$

This produces a Riemann surface Σ_t . Note that Σ_t also depends on the positions of the punctures, but the dependence is not written for simplicity.

In the following, we consider the following fixed domains in all Σ_t :

$$U_{k,\delta} = \{z \in \hat{\mathbb{C}}_k : |u_{k,\pm}^\circ(z)| > \delta/2, |v_{k,\pm}^\circ(z)| > \delta/2\}$$

and $U_\delta = \bigsqcup_{k=1}^n U_{k,\delta}$. For $1 \leq k \leq n$, we denote $0_k \in U_{k,\delta}$ the origin point in $\hat{\mathbb{C}}_k$, which will be used as the starting point for the integration defining the Weierstrass parameterization of the Scherk surface \mathcal{S}_k .

3.2. Weierstrass data. We construct a conformal minimal immersion using the Weierstrass parameterization in the form

$$z \mapsto \operatorname{Re} \int^z (\Phi_1, \Phi_2, \Phi_3) = \operatorname{Re} \int^z \Phi,$$

where $\Phi = (\Phi_1, \Phi_2, \Phi_3)$ are holomorphic 1-forms on Σ_t . At $t = 0$, Φ extend holomorphically to so called *regular 1-forms* on the noded Riemann surface Σ_0 . That means, they are holomorphic away from the nodes, with simple poles at the punctures, and opposite residues at $p_{s,k}$ and $q_{s,k+1}$. Moreover, Φ are subject to a conformal condition

$$(3) \quad Q := \Phi_1^2 + \Phi_2^2 + \Phi_3^2 = 0.$$

Note that Q is a holomorphic quadratic differential on Σ_t .

For the surface to be well defined, we need to solve the period problems. We will consider two groups of cycles on Σ_t .

For each $1 \leq k \leq n$ and $s = \pm$, let $A_{s,k}$ denote a small counterclockwise circle in $U_{k,\delta}$ around $p_{s,k}$; it is homologous in Σ_t to a clockwise circle in $U_{k+1,\delta}$ around $q_{s,k+1}$. Let us write the periods in the vector form

$$\int_{A_{s,k}} \Phi = 2\pi i(\mathbf{f}_{s,k} - i\mathbf{x}_{s,k}).$$

By the Residue Theorem, it is necessary that

$$(4) \quad \mathbf{f}_{+,k} + \mathbf{f}_{-,k} = \mathbf{f}_{+,k+1} + \mathbf{f}_{-,k+1},$$

$$(5) \quad \mathbf{x}_{+,k} + \mathbf{x}_{-,k} = \mathbf{x}_{+,k+1} + \mathbf{x}_{-,k+1}.$$

By [6, Proposition 4.2] (see also [10, Theorem 8.2]), these equations guarantee the existence of unique regular 1-forms $\Phi(t)$ on Σ_t . Moreover, the restriction of $\Phi(t)$ to U_δ depends holomorphically on t in a neighborhood of 0.

The A-period problem requires that

$$\mathbf{x}_{s,k} = s\mathbf{T}_{\varsigma(k)}(1 + \Lambda_{\varsigma(k)}\tau_{\max})$$

where \mathbf{T}_1 and \mathbf{T}_2 are the initial horizontal periods that we fixed at the beginning of the section, and $\tau_{\max} = \exp(-\ell_{\max}^\circ/\varepsilon^2)$. So Eq. (5) is already solved. Then Φ are uniquely determined by \mathbf{f} subject to Eq. (4), which we refer to as the *Balance Equation*.

More explicitly, at $\varepsilon = 0$ and the central value of all parameters, we have in $\hat{\mathbb{C}}_i$

$$(6) \quad \begin{aligned} \Phi_1^\circ &= -\frac{i \cos(\theta_{\varsigma(k)})}{z - p_{+,k}^\circ} dz - \frac{i \cos(\theta_{\varsigma(k+1)})}{z - q_{-,k}^\circ} dz + \frac{i \cos(\theta_{\varsigma(k)})}{z - p_{-,k}^\circ} dz + \frac{i \cos(\theta_{\varsigma(k+1)})}{z - q_{+,k}^\circ} dz, \\ \Phi_2^\circ &= -\frac{i \sin(\theta_{\varsigma(k)})}{z - p_{+,k}^\circ} dz - \frac{i \sin(\theta_{\varsigma(k+1)})}{z - q_{-,k}^\circ} dz + \frac{i \sin(\theta_{\varsigma(k)})}{z - p_{-,k}^\circ} dz + \frac{i \sin(\theta_{\varsigma(k+1)})}{z - q_{+,k}^\circ} dz, \\ \Phi_3^\circ &= \frac{1}{z - p_{+,k}^\circ} dz - \frac{1}{z - q_{-,k}^\circ} dz + \frac{1}{z - p_{-,k}^\circ} dz - \frac{1}{z - q_{+,k}^\circ} dz. \end{aligned}$$

In other words, Φ° is precisely the Weierstrass data of the Scherk surface \mathcal{S}_k as we want.

Let us now consider the period problems over the other group of cycles. For every $1 \leq k \leq n$, $s = \pm$ and $t_{s,k} \neq 0$, let $B_{s,k}$ be the concatenation of

- (1) a path in $U_{k,\delta}$ from 0_k to $u_{s,k} = \delta$,
- (2) the path parameterized by $u_{s,k} = \delta^{1-2\tau} (t_{s,k})^\tau$ for $\tau \in [0, 1]$, from $u_{s,k} = \delta$ to $u_{s,k} = t_{s,k}/\delta$, which is identified with $v_{s,k+1} = \delta$, and
- (3) a path in $U_{k+1,\delta}$ from $v_{s,k+1} = \delta$ to 0_{k+1} .

Again for $1 \leq k \leq n$, let B_k denote the concatenation

$$B_k = B_{+,k} * (-B_{-,k}),$$

which is a cycle in Σ_t that passes through two punctures. We also need to consider the cycle

$$B = B_{+,1} * B_{+,1} * \cdots * B_{+,n}.$$

We need to solve the following B-period problem:

$$(7) \quad \operatorname{Re} \int_{B_k} \Phi = 0,$$

$$(8) \quad \operatorname{Re} \int_B \Phi = (\mathbf{T}_3 + (\Psi_1 \Lambda_1 \mathbf{T}_1 + \Psi_2 \Lambda_2 \mathbf{T}_2) \tau_{\max}, 1/\varepsilon^2),$$

where L , \mathbf{T}_3 , Ψ_1 and Ψ_2 were defined in the Introduction.

3.2.1. Dimension count. Let us perform a dimension count before proceeding further. We have

- $6n$ real parameters $\mathbf{f}_{s,k}$.
- $2n$ complex parameters $t_{s,k}$.
- Up to Möbius transforms, we may fix three punctures on $\hat{\mathbb{C}}_k$ for each k , leaving n free complex parameters, say $p_{+,k}$.
- The shape parameters for the 3-torus. Up to Euclidean similarities, the shape is determined by five parameters, namely ε , $\Lambda_1 - \Lambda_2$, Ψ_1 , Ψ_2 , and $\theta_1 - \theta_2$.

So we have $12n + 5$ real parameters. Let us now count the equations.

- The balancing equations (4) consists of $3(n - 1)$ real equations.
- The B-period problems (7) and (8) consist of $3(n + 1)$ real equations.
- The conformality equations (3) involve quadric differentials hence contain $3g - 3 = 3n$ complex equations.

Hence there are $12n$ real equations. This is five less than the number of parameters, so 5-parameter families are expected out of our construction.

3.3. Using the Implicit Function Theorem.

3.3.1. Conformality equations. At $\varepsilon = 0$ and the central value of all parameters, Φ_3° has 4 simple poles in $\hat{\mathbb{C}}_k$, hence 2 zeros. From the explicit expression (6), we know that the two zeroes are $\zeta_{k,0}^\circ = 0_k$ and $\zeta_{k,\infty}^\circ = \infty_k$. When the parameters are close to their central value, Φ_3 has simple zeroes $\zeta_{k,0}$ and $\zeta_{k,\infty}$ respectively close to 0_k and ∞_k .

The conformality equation will be converted into the following equations:

$$(9) \quad \int_{A_{s,k}} \frac{Q}{\Phi_3} = 0,$$

$$(10) \quad \operatorname{Res} \left(\frac{Q}{\Phi_3}, \zeta_{k,0} \right) = 0.$$

for $1 \leq k \leq n$ and $s = \pm$. The same argument as in [2] applies to prove the following statements.

Proposition 5. *The conformality equation (3) is solved if the equations (4), (9), and (10) are solved.*

Proposition 6. *For (t, \mathbf{f}) in a neighborhood of $(0, \mathbf{f}^\circ)$, there exists $p = (p_{s,k})$ depending analytically on (t, \mathbf{f}) , such that the conformality equations (10) are solved, and $p_{s,k}(0, \mathbf{f}^\circ) = p_{s,k}^\circ$.*

From now on, we assume that the punctures p are given by Proposition 6.

For $j = 1, 2$, let \mathbf{T}_j^\perp be the unit vector obtained by anticlockwise rotation of \mathbf{T}_j by $\pi/2$. We decompose $\mathbf{f}_{s,k}$ into

$$\mathbf{f}_{s,k} = \alpha_{s,k}(\mathbf{T}_{\varsigma(k)}, 0) + \beta_{s,k}(\mathbf{T}_{\varsigma(k)}^\perp, 0) + \gamma_{s,k}(0, 0, 1).$$

We also write $\rho_{s,k} = \sqrt{(\beta_{s,k})^2 + (\gamma_{s,k})^2}$ and

$$(11) \quad t_{s,k} = -\exp\left(-\ell_{s,k}\varepsilon^{-2} + i\psi_{s,k}\right).$$

The central values of $(\ell_{s,k}, \psi_{s,k})$ are $(\ell_k^\circ, \psi_k^\circ)$. We often change to the variable $\zeta_{s,k}$ where $\ell_{s,k} = \ell_k^\circ + \varepsilon^2 \zeta_{s,k}$. So $\zeta_{s,k}^\circ = \partial \ell_{s,k} / \partial (\varepsilon^2)$ at $\varepsilon = 0$.

The next proposition is the key ingredient of our construction. It is the only place where a deformation in the horizontal lattice can play a role. This is the reason for our definition (1) of the deformed horizontal lattice.

Proposition 7. *For (t, β) in a neighborhood of $(0, 0)$, there exist unique values of α and ρ , depending real-analytically on (t, β) , such that the equations (9) are solved. At $t_{s,k} = 0$ we have, no matter the values of other parameters, that*

$$(12) \quad \rho_{s,k} = 1 \quad \text{and} \quad \alpha_{s,k} = 0.$$

Moreover, at $(t, \beta) = (0, 0)$, we have the Wirtinger derivatives

$$(13) \quad \frac{\partial \rho_{s,k}}{\partial t_{s,k}} = \Xi_{s,k} \quad \text{and} \quad \frac{\partial \alpha_{s,k}}{\partial t_{s,k}} = s\Xi_{s,k}i.$$

where $\Xi_{s,k} = -2$ when $\ell_k^\circ < \ell_{max}^\circ$, and

$$\Xi_{s,k} = -2 - \frac{\Lambda_{\varsigma(k)} \exp(\zeta_{s,k}^\circ - i\psi_{s,k})}{2}$$

when $\ell_{s,k}^\circ = \ell_{max}^\circ$.

Proof. Define for $1 \leq k \leq n$

$$\mathcal{E}_{s,k}(t, \alpha, \beta, \rho) = \frac{1}{2\pi i} \int_{A_{s,k}} \frac{Q}{\Phi_3}.$$

Assume that $t_{s,k} = 0$. Then Φ_1 , Φ_2 , and Φ_3 have a simple pole at $p_{s,k}$, so Q/Φ_3 has a simple pole at $p_{s,k}$ and, by the Residue Theorem

$$\mathcal{E}_{s,k} |_{t_{s,k}=0} = \frac{(\mathbf{f}_{k,s}^\circ - i\mathbf{x}_{k,s}^\circ)^2}{\gamma_{s,k}} = \frac{(\alpha_{s,k})^2 + (\rho_{s,k})^2 - 2is\alpha_{s,k} - 1}{\gamma_{s,k}}.$$

So the solution to (9) is $(\alpha_{s,k}, \rho_{s,k}) = (0, 1)$, no matter the values of the other parameters. This proves (12).

We compute the partial derivatives of $\mathcal{E}_{s,k}$ with respect to $\alpha_{s,k}, \rho_{s,k}$ at $(t, \alpha, \beta, \rho) = (0, 0, 0, 1)$:

$$(14) \quad \frac{\partial \mathcal{E}_{s,k}}{\partial \alpha_{s,k}} = -2is, \quad \frac{\partial \mathcal{E}_{s,k}}{\partial \rho_{s,k}} = 2.$$

So the existence and uniqueness statement of the proposition follows from the Implicit Function Theorem.

To prove the last point, we need to compute the partial derivative of $\mathcal{E}_{s,k}$ with respect to $t_{s,k}$ at $(t, \alpha_{s,k}, \beta_{s,k}, \rho_{s,k}) = (0, 0, 0, 1)$. The computation is similar to

those in [2]. By the Residue Theorem and [9, Lemma 3] (see also [2, Lemma 8.2]), we have

$$\begin{aligned}
\frac{\partial \mathcal{E}_{s,k}}{\partial t_{s,k}} &= \text{Res} \left(\sum_{j=1}^3 2 \frac{\Phi_j^\circ}{\Phi_3^\circ} \frac{\partial \Phi_j}{\partial t_{s,k}}, p_{s,k}^\circ \right) \\
&= -2 \sum_{j=1}^3 \text{Res} \left(\frac{\Phi_j^\circ}{\Phi_3^\circ} \frac{du_{s,k}}{(u_{s,k})^2}, p_{s,k}^\circ \right) \text{Res} \left(\frac{\Phi_j^\circ}{v_{s,k+1}}, q_{s,k+1}^\circ \right) \\
(15) \quad &= -2 \sum_{j=1}^3 \text{Res} \left(\frac{\Phi_j^\circ}{u_{s,k}}, p_{s,k}^\circ \right) \text{Res} \left(\frac{\Phi_j^\circ}{v_{s,k+1}}, q_{s,k+1}^\circ \right) \\
(16) \quad &\quad + 2 \text{Res} \left(\frac{\Phi_3^\circ}{u_{s,k}}, p_{s,k}^\circ \right) \sum_{j=1}^3 \text{Res} \left(\Phi_j^\circ, p_{s,k}^\circ \right) \text{Res} \left(\frac{\Phi_j^\circ}{v_{s,k+1}}, q_{s,k+1}^\circ \right).
\end{aligned}$$

Since $Q^\circ = 0$, we have

$$(17) \quad \text{Res} \left(\frac{u_{s,k} Q^\circ}{du_{s,k}}, p_{s,k}^\circ \right) = \sum_{j=1}^3 \text{Res} \left(\Phi_j^\circ, p_{s,k}^\circ \right)^2 = 0,$$

$$(18) \quad \text{Res} \left(\frac{Q^\circ}{dv_{s,k}}, q_{s,k}^\circ \right) = 2 \sum_{j=1}^3 \text{Res} \left(\Phi_j^\circ, q_{s,k}^\circ \right) \text{Res} \left(\frac{\Phi_j^\circ}{v_{s,k}}, q_{s,k}^\circ \right) = 0.$$

Because $\text{Res} \left(\Phi_j^\circ, q_{s,k+1}^\circ \right) = -\text{Res} \left(\Phi_j^\circ, p_{s,k}^\circ \right)$, Eq. (18) implies that the term (16) vanishes. Note that

$$\frac{1}{\sqrt{2}} \text{Res} \left(\Phi^\circ, p_{s,k}^\circ \right), \quad \frac{1}{\sqrt{2}} \text{Res} \left(\overline{\Phi^\circ}, p_{s,k}^\circ \right), \quad N^\circ(p_{s,k}^\circ)$$

form an orthonormal basis of \mathbb{C}^3 for the standard hermitian product $\langle \cdot, \cdot \rangle_H$. After recalling the definition and value of Υ in Section 2, we decompose in this basis

$$\begin{aligned}
\text{Res} \left(\frac{\Phi^\circ}{u_{s,k}}, p_{s,k}^\circ \right) &= \frac{1}{2} \left\langle \text{Res} \left(\Phi^\circ, p_{s,k}^\circ \right), \text{Res} \left(\frac{\Phi^\circ}{u_{s,k}}, p_{s,k}^\circ \right) \right\rangle_H \text{Res} \left(\Phi^\circ, p_{s,k}^\circ \right) \\
&\quad + \left\langle N^\circ(p_{s,k}^\circ), \text{Res} \left(\frac{\Phi^\circ}{u_{s,k}}, p_{s,k}^\circ \right) \right\rangle_H N^\circ(p_{s,k}^\circ) \\
&= \frac{1}{2} \left\langle \text{Res} \left(\Phi^\circ, p_{s,k}^\circ \right), \text{Res} \left(\frac{\Phi^\circ}{u_{s,k}}, p_{s,k}^\circ \right) \right\rangle_H \text{Res} \left(\Phi^\circ, p_{s,k}^\circ \right) + 2N^\circ(p_{s,k}^\circ).
\end{aligned}$$

Here, the component on $\text{Res} \left(\overline{\Phi^\circ}, p_{s,k}^\circ \right)$ vanishes because of (18). In the same way, after recalling that $N^\circ(p_{s,k}^\circ) = N^\circ(q_{s,k+1}^\circ)$,

$$\begin{aligned}
\text{Res} \left(\frac{\Phi^\circ}{v_{s,k+1}}, q_{s,k+1}^\circ \right) &= \\
&\quad \frac{1}{2} \left\langle \text{Res} \left(\Phi^\circ, p_{s,k}^\circ \right), \text{Res} \left(\frac{\Phi^\circ}{v_{s,k+1}}, q_{s,k+1}^\circ \right) \right\rangle_H \text{Res} \left(\Phi^\circ, p_{s,k}^\circ \right) - 2N^\circ(p_{s,k}^\circ).
\end{aligned}$$

Hence by Equation (15)

$$\frac{\partial \mathcal{E}_{s,k}}{\partial t_{s,k}} = -2 \left\langle \overline{\text{Res} \left(\frac{\Phi^\circ}{u_{s,k}}, p_{s,k}^\circ \right)}, \text{Res} \left(\frac{\Phi^\circ}{v_{s,k+1}}, q_{s,k+1}^\circ \right) \right\rangle_H = 8.$$

Since $\mathbf{x}_{s,k}$ could also depend on $t_{s,k}$ (through τ_{\max}), we still need to compute

$$(19) \quad \text{Res} \left(2 \frac{\Phi_1^\circ}{\Phi_3^\circ} \frac{\partial \Phi_1}{\partial x_{s,k}} \frac{\partial x_{s,k}}{\partial t_{s,k}}, p_{s,k}^\circ \right) + \text{Res} \left(2 \frac{\Phi_2^\circ}{\Phi_3^\circ} \frac{\partial \Phi_2}{\partial y_{s,k}} \frac{\partial y_{s,k}}{\partial t_{s,k}}, p_{s,k}^\circ \right),$$

where $\mathbf{x}_{s,k} = (x_{s,k}, y_{s,k}, 0)$. The computation is dependent on ℓ_k° .

Recall that $\tau_{\max} = \exp(-\ell_{\max}^\circ/\varepsilon^2)$. When $\ell_k^\circ < \ell_{\max}^\circ$, $\partial \mathbf{x}_{s,k}/\partial t_{s,k} = 0$, hence (19) vanishes. In this case, taking the total derivative of $\mathcal{E}_{s,k}$ against $t_{s,k}$ gives

$$(20) \quad 8 - 2is \frac{\partial \alpha_{s,k}}{\partial t_{s,k}} + 2 \frac{\partial \rho_{s,k}}{\partial t_{s,k}} = 0.$$

On the other hand, since $\mathcal{E}_{s,k}$ is holomorphic in $t_{s,k}$, we have

$$2is \frac{\partial \alpha_{s,k}}{\partial t_{s,k}} + 2 \frac{\partial \rho_{s,k}}{\partial t_{s,k}} = 0.$$

Hence the Wirtinger derivatives

$$\frac{\partial \rho_{s,k}}{\partial t_{s,k}} = -2 \quad \text{and} \quad \frac{\partial \alpha_{s,k}}{\partial t_{s,k}} = -2is.$$

When $\ell_k^\circ = \ell_{\max}^\circ$, $\partial \mathbf{x}_{s,k}/\partial \tau_{\max} = s \Lambda_{\varsigma(k)} \mathbf{T}_{\varsigma(k)}$ and

$$\frac{\partial \tau_{\max}}{\partial t_{s,k}} = \lim_{\varepsilon \rightarrow 0} \frac{\tau_{\max}}{t_{s,k}} = -\exp(\zeta_{s,k}^\circ - i\psi_{s,k}),$$

So (19) equals

$$\begin{aligned} & 2is \exp(\zeta_{s,k}^\circ - i\psi_{s,k}) \Lambda_{\varsigma(k)} \mathbf{T}_{\varsigma(k)} \cdot \left(\operatorname{Res} \left(\frac{\Phi_1^\circ}{\Phi_3^\circ} \frac{1}{u_{s,k}}, p_{s,k}^\circ \right), \operatorname{Res} \left(\frac{\Phi_2^\circ}{\Phi_3^\circ} \frac{1}{u_{s,k}}, p_{s,k}^\circ \right) \right) \\ &= 2is \exp(\zeta_{s,k}^\circ - i\psi_{s,k}) \Lambda_{\varsigma(k)} \mathbf{T}_{\varsigma(k)} \cdot (-is \mathbf{T}_{\varsigma(k)}) = 2 \exp(\zeta_{s,k}^\circ - i\psi_{s,k}) \Lambda_{\varsigma(k)}. \end{aligned}$$

In this case, taking the total derivative of $\mathcal{E}_{s,k}$ against $t_{s,k}$ gives

$$(21) \quad 8 + 2\Lambda_{\varsigma(k)} \exp(\zeta_{s,k}^\circ - i\psi_{s,k}) - 2is \frac{\partial \alpha_{s,k}}{\partial t_{s,k}} + 2 \frac{\partial \rho_{s,k}}{\partial t_{s,k}} = 0.$$

On the other hand, since $\mathcal{E}_{s,k}$ and τ_{\max} are holomorphic in $t_{s,k}$, we have

$$(22) \quad 2is \frac{\partial \alpha_{s,k}}{\partial t_{s,k}} + 2 \frac{\partial \rho_{s,k}}{\partial t_{s,k}} = 0.$$

Hence the Wirtinger derivatives

$$\begin{aligned} \frac{\partial \rho_{s,k}}{\partial t_{s,k}} &= -2 - \frac{\Lambda_{\varsigma(k)} \exp(\zeta_{s,k}^\circ - i\psi_{s,k})}{2} = \Xi_{s,k}, \\ \frac{\partial \alpha_{s,k}}{\partial t_{s,k}} &= s \left(-2 - \frac{\Lambda_{\varsigma(k)} \exp(\zeta_{s,k}^\circ - i\psi_{s,k})}{2} \right) i = s \Xi_{s,k} i. \end{aligned}$$

□

In other words, we have

$$(23) \quad \alpha_{s,k} = 4s \operatorname{Im} t_{s,k} + o(|t_{s,k}|),$$

$$(24) \quad \rho_{s,k} = \begin{cases} 1 - 4 \operatorname{Re} t_{s,k} + o(|t_{s,k}|), & \ell_{s,k}^\circ < \ell_{\max}^\circ, \\ 1 - 4 \operatorname{Re} t_{s,k} + \Lambda_{\varsigma(k)} \exp(\zeta_{s,k}^\circ) |t_{s,k}| + o(|t_{s,k}|), & \ell_{s,k}^\circ = \ell_{\max}^\circ. \end{cases}$$

Or more concisely

$$\alpha_{s,k} = -4s \sin(\psi_{s,k}) |t_{s,k}|, \quad \rho_{s,k} = 1 + K_{s,k} |t_{s,k}| + o(|t_{s,k}|),$$

where

$$K_{s,k} = \begin{cases} 4 \cos(\psi_{s,k}) + \Lambda_{\varsigma(k)} \exp(\zeta_{s,k}^\circ), & \ell_k^\circ = \ell_{\max}^\circ, \\ 4 \cos(\psi_{s,k}), & \ell_k^\circ < \ell_{\max}^\circ, \end{cases}$$

From now on, we assume that the parameters α and ρ are given by Proposition 7.

3.3.2. *B-period problem.*

Proposition 8. *For $(\varepsilon, \ell_{+,k}, \psi_{+,k}, \beta_{+,k})$ in a neighborhood of $(0, \ell_k^\circ, \psi_k^\circ, 0)$, there exist unique values for $(\ell_{-,k})$, $(\psi_{-,k})$, and $(\beta_{-,k})$, depending smoothly on $(\varepsilon, \ell_{+,k}, \psi_{+,k})$, such that the *B-period equations* (7) are solved. Moreover, at $\varepsilon = 0$, we have $\ell_{+,k} = \ell_{-,k}$, $\psi_{+,k} = -\psi_{-,k}$, and $\beta_{+,k} = \beta_{-,k}$.*

Proof. By [8, Lemma 1] (see also Appendix of [2]), the difference

$$(25) \quad \left(\int_{B_{s,k}} \Phi \right) - (\mathbf{f}_{s,k} - i\mathbf{x}_{s,k}) \log t_{s,k}$$

extends holomorphically to $t_{s,k} = 0$. Moreover, its value at $t = 0$ is equal to

$$\begin{aligned} & \lim_{z \rightarrow p_{s,k}} \left[\left(\int_{0_k}^z \Phi \right) - (\mathbf{f}_{s,k} - i\mathbf{x}_{s,k}) \log u_{s,k}(z) \right] \\ & - \lim_{z \rightarrow q_{s,k+1}} \left[\left(\int_{0_{k+1}}^z \Phi \right) - (\mathbf{f}_{s,k+1} - i\mathbf{x}_{s,k+1}) \log v_{s,k+1}(z) \right], \end{aligned}$$

whose real part, by the computations in Section 2, equals

$$(0, 0, -2 \log(\sin \theta \cos \theta)).$$

Recall that

$$\mathbf{f}_{s,k} = \alpha_{s,k}(\mathbf{T}_{\varsigma(k)}, 0) + \beta_{s,k}(\mathbf{T}_{\varsigma(k)}^\perp, 0) + \gamma_{s,k}(0, 0, 1)$$

and that $\alpha_{s,k} = O(\exp(-\ell_{s,k}/\varepsilon^2))$. Then, as $t \rightarrow 0$, we have

$$\begin{aligned} & (\mathbf{T}_{\varsigma(k)}, 0) \cdot \left(\int_{B_k} \Phi \right) \rightarrow (\psi_{-,k} + \psi_{+,k}) + \lim_{\varepsilon \rightarrow 0} \left(\alpha_{-,k} \frac{\ell_{-,k}}{\varepsilon^2} - \alpha_{+,k} \frac{\ell_{+,k}}{\varepsilon^2} \right) = (\psi_{-,k} + \psi_{+,k}), \\ & \varepsilon^2(\mathbf{T}_{\varsigma(k)}^\perp, 0) \cdot \left(\int_{B_k} \Phi \right) \rightarrow (\beta_{-,k} \ell_{-,k} - \beta_{+,k} \ell_{+,k}), \\ & \varepsilon^2(0, 0, 1) \cdot \left(\int_{B_k} \Phi \right) \rightarrow (\ell_{-,k} \gamma_{-,k} - \ell_{+,k} \gamma_{+,k}). \end{aligned}$$

The period problem requires all these to vanish at $\varepsilon = 0$. This is solved at $\varepsilon = 0$ with

$$\ell_{-,k} = \ell_{+,k}, \quad \beta_{-,k} = \beta_{+,k}, \quad \psi_{-,k} = -\psi_{+,k},$$

and the Proposition easily follows from the Implicit Function Theorem. \square

From now on, we assume that the parameters ℓ_- , ψ_- , and β_- are given by Proposition 8.

3.3.3. *Balance condition.* Recall that

$$K_k = \begin{cases} 4 \cos(\psi_k) + \Lambda_{\varsigma(k)} \exp(\zeta_k^\circ), & \ell_k^\circ = \ell_{\max}^\circ, \\ 4 \cos(\psi_k), & \ell_k^\circ < \ell_{\max}^\circ, \end{cases}$$

Proposition 9. *For the balance equations (4) to be solved at $\varepsilon = 0$, it is necessary that the central values ℓ_k° , ψ_k° for $\ell_{+,k}$, $\psi_{+,k}$ only depend on the parity of k . That is,*

$$\ell_k^\circ = \ell_{\varsigma(k)}^\circ, \quad \psi_k^\circ = \psi_{\varsigma(k)}^\circ.$$

If this is indeed the case, then for ε in a neighborhood of 0, there exist unique values for $\ell_{+,1}$, ψ_+ and β_+ , depending smoothly on ε and other parameters, such that

$$(26) \quad \psi_{+,1} \rightarrow \psi_1^\circ = 2\Psi_1/n, \quad \psi_{+,2} \rightarrow \psi_2^\circ = 2\Psi_2/n, \quad \ell_{+,1} + \ell_{+,2} \rightarrow \ell_1^\circ + \ell_2^\circ = 2/n$$

*as $\varepsilon \rightarrow 0$, and the *B-period problem* (8) as well as the horizontal components of the balance equation (4) are solved. Moreover, as $\varepsilon \rightarrow 0$, we have*

$$(27) \quad \zeta_{+,1} + \zeta_{+,2} = 4 \log(\sin \theta \cos \theta).$$

Proof. Define $\tau_k = \exp(-\ell_k^\circ/\varepsilon^2)$. We want $(\ell_+, \psi_+)(0) = (\ell^\circ, \psi^\circ)$. From (23), (24), Proposition 8 and the definition of t , we know that

$$\begin{aligned}\lim_{\tau_k \rightarrow 0} \frac{\alpha_{s,k}}{\tau_k} &= -4 \sin(\psi_k) \exp(-\zeta_{+,k}^\circ), \\ \lim_{\tau_k \rightarrow 0} \frac{\rho_{s,k} - 1}{\tau_k} &= K_k \exp(-\zeta_{+,k}^\circ),\end{aligned}$$

both are independent of s . Since the forces on the odd (resp. even) levels are decomposed into the same basis, the balance equations (4) require, in particular, that

$$(28) \quad \frac{1}{\tau_k} (\alpha_{+,k}, \rho_{+,k} - 1) = \frac{1}{\tau_k} (\alpha_{+,\varsigma(k)}, \rho_{+,\varsigma(k)} - 1),$$

These equations, depending on the parity of k , can be solved at $\varepsilon = 0$ only if $\ell_k^\circ = \ell_{\varsigma(k)}^\circ$. To see this, assume without loss of generality that $\ell_k^\circ < \ell_{\varsigma(k)}^\circ$, then $\tau_{\varsigma(k)} = o(\tau_k)$. Consequently, the left side of (28) extends to $\varepsilon = 0$ with a nonzero value, while the right side tends to 0. Now, if $\ell_k^\circ = \ell_{\varsigma(k)}^\circ$, then (28) is solved at $\varepsilon = 0$ by $\psi_k^\circ = \psi_{\varsigma(k)}^\circ$. We have thus proved the necessity that ℓ_k° and ψ_k° both depend on the parity of k .

Now assume that ℓ° and ψ° both depend on the parity of k . By the same argument as in the previous proof, we have

$$\left(\int_B \Phi_1, \int_B \Phi_2, \varepsilon^2 \int_B \Phi_3 \right) \rightarrow \frac{n}{2} (\psi_{+,1} \mathbf{T}_1, \psi_{+,2} \mathbf{T}_2, \ell_{+,1} + \ell_{+,2}).$$

So the B-period (8) is solved at $\varepsilon = 0$ by the central values given in (26), and the proposition follows from the Implicit Function Theorem. Moreover, as $\varepsilon \rightarrow 0$, we have

$$\frac{\frac{2\varepsilon^2}{n} \int_B \Phi_3 - (\ell_1^\circ + \ell_2^\circ)}{\varepsilon^2} \rightarrow \zeta_{+,1} + \zeta_{+,2} - 4 \log(\sin \theta \cos \theta),$$

which should vanish to close the periods.

The balance equations (4) require that the force \mathbf{f} is independent of k . Consequently α , β , and γ all depend on the parity of k . So the balance equations reduce to

$$(29) \quad \alpha_{+,1} \mathbf{T}_1 + \beta_{+,1} \mathbf{T}_1^\perp = \alpha_{+,2} \mathbf{T}_2 + \beta_{+,2} \mathbf{T}_2^\perp,$$

$$(30) \quad \gamma_{+,1} = \gamma_{+,2}.$$

Note that \mathbf{T}_1 and \mathbf{T}_2 are linearly independent, and so are \mathbf{T}_1^\perp and \mathbf{T}_2^\perp . Hence for any $\alpha_{+,1}$ and $\alpha_{+,2}$, there exists unique $\beta_{+,1}$ and $\beta_{+,2}$ that solves the horizontal balance (29). In fact, an elementary computation gives

$$\beta_{+,1} = \frac{\alpha_{+,1}}{\tan(2\theta)} - \frac{\alpha_{+,2}}{\sin(2\theta)}, \quad \beta_{+,2} = \frac{\alpha_{+,1}}{\sin(2\theta)} - \frac{\alpha_{+,2}}{\tan(2\theta)}.$$

Note that $\beta_{+,1}^2 - \beta_{+,2}^2 = \alpha_{+,2}^2 - \alpha_{+,1}^2$. \square

From now on, we assume that the parameters $\ell_{+,1}$, ψ_+ , and β_+ are given by Proposition 9.

The remaining parameters are $\ell_{+,2}$ (or $\zeta_{+,2}$) and the lattice shape parameters, including ε , $\theta_{1,2}$, $\psi_{1,2}$, and $\Lambda_{1,2}$. Usually, we would use the Implicit Function Theorem to solve $\ell_{+,2}$ of $\zeta_{+,2}$ as a function of the shape parameters. But such a solution may not exist for a given $\Lambda_{1,2}$; see Remark 2 later. In the following, we will instead solve $\Lambda_1 - \Lambda_2$ as a function of $\ell_{+,2}$ and other shape parameters.

Proposition 10. *If ℓ_k° , ψ_k° depend only on the parity of k and $K_k \neq 0$ for all $1 \leq k \leq n$, then ℓ° is necessarily constant for the balance equations (4) to be solved. If this is indeed the case, then for ε in a neighborhood of 0, there exists unique*

values for $\Lambda_2 - \Lambda_1$, depending smoothly on other parameters, such that the vertical component of the balance equation (30) is solved.

Proof. Note that

$$|\mathbf{f}_{+,k}|^2 - 1 = \rho_{+,k}^2 + \alpha_{+,k}^2 - 1 = 2K_k \exp(-\zeta_{+,k})\tau_k + o(\tau_k).$$

The balance equation (4) implies that

$$\frac{|\mathbf{f}_{+,1}|^2 - 1}{\tau_2} = \frac{|\mathbf{f}_{+,2}|^2 - 1}{\tau_2}.$$

But if $\ell_{\max}^\circ = \ell_1^\circ > \ell_2^\circ$, $\tau_1 = o(\tau_2)$, then as $\varepsilon \rightarrow 0$, the left hand side vanishes but the right hand side is $K_2 \exp(-\zeta_{+,2}) \neq 0$. This proves that ℓ° must be constant.

In this case, we now solve the vertical balance (30). Note that

$$\gamma_{+,k} - 1 = \sqrt{\rho_{+,k}^2 - \beta_{+,k}^2} - 1 = K_k \exp(-\zeta_{+,k})\tau_k + o(\tau_k).$$

Now that $\tau_1 = \tau_2 = \tau_k$, the vertical balance (30) is solved at $\varepsilon = 0$ if

$$\exp(-\zeta_{+,k})K_k = 4 \cos(\psi_k^\circ) \exp(-\zeta_{+,k}) + \Lambda_{\varsigma(k)}$$

is a constant independent of k . This implies that $\zeta_{+,k} = \zeta_{+,\varsigma(k)}$ depend on the parity of k and

$$(31) \quad 4 \cos(\psi_1^\circ) \exp(-\zeta_{+,1}) - \cos(\psi_2^\circ) \exp(-\zeta_{+,2}) + \Lambda_1 - \Lambda_2 = 0.$$

The proposition follows since this balance equation is linear in $\Lambda_2 - \Lambda_1$. \square

Remark 1. We are not able to conclude a constant ℓ° if $K_k = 0$ for some k . We believe that in this case, the surfaces converge to KMR examples, so a future construction that glues KMR surfaces into TPMSSs is expected.

Remark 2. The equations (27) and (31) give a quadratic equation of $\exp(-\zeta_{+,2})$ at $\varepsilon = 0$. But the equation may not have a positive real solution. This is why we are not able to solve $\zeta_{+,2}$ as a function of the shape parameters. For instance, for the Scherk limit oP surfaces, we have $\psi_1^\circ = 0$ and $\psi_2^\circ = \pi$ hence $\cos(\psi_1^\circ) = -\cos(\psi_2^\circ) = 1$; see Figure 1 middle. But then, if we insist $\Lambda_1 = \Lambda_2 = 0$, (31) would have no solution at all. In other words, the shape of the lattice can not be arbitrary. In the case of oP, the particular choice of phase forces a change in the aspect ratio of the horizontal lattice.

Finally, by the same argument as in [2] and using Eq. (25), one proves that the immersion given by the Weierstrass Representation is a regular embedding and has the geometry described in the Introduction.

4. PROOFS OF MAIN RESULTS

We now prove the Main Theorem 1.

4.1. The special case of triangular lattice.

Proof of Lemma 2. Assume that the upward (resp. downward) ends of \mathcal{S}_k are parallel to unit vectors \mathbf{T}_k (resp. \mathbf{T}_{k-1}), and that $\langle 2\pi\mathbf{T}_{k-1}, 2\pi\mathbf{T}_k \rangle$ are the periods of \mathcal{S}_k . Here we adopt the convention that \mathbf{T}_{k-1} and \mathbf{T}_k form an acute angle. Since adjacent ends can not be parallel, we have $\mathbf{T}_k \neq \mathbf{T}_{k-1}$. For the sake of contradiction, assume that the direction of ends does *not* depend on the parity of k . Then there must be three consecutive integers, say $i-1, i, i+1$, such that $\mathbf{T}_{i-1}, \mathbf{T}_i, \mathbf{T}_{i+1}$ are pairwise non-parallel.

Let \mathbb{T}_0^2 be the limit horizontal lattice as $\varepsilon \rightarrow 0$. Without loss of generality, we may assume that $\mathbb{T}_0^2 = \mathbb{R}^2 / \langle 2\pi\mathbf{T}_{i-1}, 2\pi\mathbf{T}_i \rangle$. But $2\pi\mathbf{T}_{i+1}$ is also a period. That is, \mathbf{T}_{i+1} is an integer combination of \mathbf{T}_i and \mathbf{T}_{i-1} . That is

$$(32) \quad \mathbf{T}_{i+1} = a\mathbf{T}_{i-1} + b\mathbf{T}_i, \quad a, b \in \mathbb{Z}.$$

Moreover, the horizontal fundamental parallelogram of \mathcal{S}_i and \mathcal{S}_{i+1} must have the same area. So the angle $\angle \widehat{\mathbf{T}_{i-1}\mathbf{T}_i}$ must equal to the angle $\angle \widehat{\mathbf{T}_i\mathbf{T}_{i+1}}$. Taking the cross product of (32) with \mathbf{T}_i , we obtain $a = -1$. But since $\mathbf{T}_{i+1} \neq \pm\mathbf{T}_{i-1}$ and they are all unit vectors, we have $0 < b < 2$, so $b = 1$.

We then conclude the relation $\mathbf{T}_{i+1} + \mathbf{T}_{i-1} = \mathbf{T}_i$ among three unit period vectors. This is only possible in a triangular lattice. \square

So, if the limit horizontal lattice is not triangular, \mathbf{T}_k must depend on the parity of k , which is the case considered in this paper.

Remark 3. In the special case of triangular limit horizontal lattice, the vertical planes can be parallel $e^{i\pi j/3}$, $j = 1, 2, 3$. This leads to a wide variety of possibilities. The simplest configuration is $\mathbf{T}_k = e^{i\pi k/3}$, $k \in \mathbb{Z}$, which gives the doubly periodic Scherk limit of a recently discovered family of TPMSs of genus 4 [5]. A similar argument as ours would prove that, whenever $\mathbf{T}_k = \mathbf{T}_{k'}$, we must have

$$\ell_k^\circ = \ell_{k'}^\circ \quad \text{and} \quad \psi_k^\circ = \psi_{k'}^\circ.$$

But with three possible directions, one may easily create very complicated sequences, even non-periodic infinite sequences. More curious is an analogy of Proposition 10. More specifically, how would the surface behave if the horizontal lattice deforms away from triangular? Although very interesting, we do not plan to discuss these examples in the current paper.

In [2], the singly periodic Scherk limit of the surfaces in [5] also stood out as a curious special case, and the behavior when the horizontal lattice deforms away from triangular was not understood either.

4.2. Otherwise, no new examples.

Proof of Theorem 3. We have shown that, for the construction to succeed, the periodic sequence of Scherk surfaces must actually have period 2. The situation is the same as if we wanted to construct TPMSs of genus 3 by gluing two Scherk surfaces. We will prove that these TPMSs of genus 3 belong to Meeks' family, characterized by an orientation-reversing translation.

The translation $\pi(\mathbf{x}_{+,1} + \mathbf{x}_{+,2}, 0)$ is orientation reversing for the Scherk surfaces. Let ϱ denote this transformation. Note that ϱ swaps $p_{\pm,k}$ and, respectively, $q_{\pm,k}$. Up to Möbius transforms, we may assume that $p_{+,k} = -p_{-,k}$. Then $\varrho(z) = -1/\bar{z}$. If our surfaces were assumed to be symmetric under ϱ , then we would automatically have

$$\mathbf{f}_{-,k} = \mathbf{f}_{+,k}, \quad t_{-,k} = \bar{t}_{+,k}.$$

All other parameters can be found using the Implicit Function Theorem as we did in the previous section.

But by the Implicit Function Theorem, the solution is unique. Hence the solution we found in the previous section must coincide with the symmetric TPMSg3 solution. In other words, the TPMSs we construct must be of genus 3 and have an orientation-reversing translational symmetry. That is, they belong to the Meeks family. \square

Remark 4. We see from Remark 2 that, near the doubly periodic Scherk boundary, the 5-parameter Meeks manifold is not parameterized by the shape of the lattice. More specifically, $\Lambda_{1,2}$ are replaced by $\partial\ell/\partial(\varepsilon^2)$ as parameters of this manifold.

Our construction for TPMSSs can easily be adapted to construct DPMSSs. It suffices to leave the four punctures $p_{\pm,n}$ and $q_{\pm,1}$ “free”. That is, they are not identified with other punctures to form any node. Equivalently, we can think of the situation as if $q_{\pm,1}$ (resp. $p_{\pm,n}$) were identified to some $p_{\pm,0} \in \mathbb{C}_0$ (resp. $q_{\pm,n+1} \in \mathbb{C}_{n+1}$) to form nodes but were never opened, i.e.

$$t_{s,0} = t_{s,n} \equiv 0$$

but $|t_{s,k}| > 0$ for $1 \leq k < n$. We are now ready to prove Theorem 4.

Proof of Theorem 4. By the computation in the proof of 7, since $t_{s,0} = t_{s,n} \equiv 0$ we have

$$\rho_{s,0} = \rho_{s,n} \equiv 1, \quad \alpha_{s,0} = \alpha_{s,n} \equiv 0.$$

By a similar argument as in the proof of 9, if $n > 2$, we must also have $t_{s,2} = 0$, which is against our assumption. This proves that $n \leq 2$. But in the cases $n = 1$ (genus 0) and $n = 2$ (genus 1), doubly periodic surfaces with Scherk ends have been fully classified [4, 7], so the surfaces we construct must be a Scherk surface or a KMR example. \square

REFERENCES

- [1] Hao Chen and Daniel Freese. Helicoids and vortices. *Proc. A.*, 478(2267):Paper No. 20220431, 18, 2022.
- [2] Hao Chen and Martin Traizet. Gluing Karcher-Scherk saddle towers I: triply periodic minimal surfaces. *J. Reine Angew. Math.*, 808:1–47, 2024.
- [3] Howard Jenkins and James Serrin. The Dirichlet problem for the minimal surface equation, with infinite data. *Bull. Amer. Math. Soc.*, 72:102–106, 1966.
- [4] Hippolyte Lazard-Holly and William H. Meeks, III. Classification of doubly-periodic minimal surfaces of genus zero. *Invent. Math.*, 143(1):1–27, 2001.
- [5] Shashank Ganesh Markande, Matthias Saba, Gerd Schroeder-Turk, and Elisabetta A. Matsumoto. A chiral family of triply-periodic minimal surfaces derived from the quartz network, 2018. Preprint arXiv:1805.07034.
- [6] Howard Masur. Extension of the Weil-Petersson metric to the boundary of Teichmuller space. *Duke Math. J.*, 43(3):623–635, 1976.
- [7] Joaquín Pérez, M. Magdalena Rodríguez, and Martin Traizet. The classification of doubly periodic minimal tori with parallel ends. *J. Differential Geom.*, 69(3):523–577, 2005.
- [8] Martin Traizet. An embedded minimal surface with no symmetries. *J. Diff. Geom.*, 60:103–153, 2002.
- [9] Martin Traizet. On the genus of triply periodic minimal surfaces. *J. Diff. Geom.*, 79(2):243–275, 2008.
- [10] Martin Traizet. Opening infinitely many nodes. *J. Reine Angew. Math.*, 684:165–186, 2013.

Email address: chenhao5@shanghaitech.edu.cn

Email address: wuyh12023@shanghaitech.edu.cn

SHANGHAI TECH UNIVERSITY, SHANGHAI, CHINA